Dynamic PDE parametric curves

Xu-Zheng Liu, Xia Cui, Guo-Qin Zheng, Jun-Hai Yong, Jia-Guang Sun

Dynamic PDE parametric curves

Xu-Zheng Liu[a, b, *], Xia Cui[c], Guo-Qin Zheng[a], Jun-Hai Yong[a], Jia-Guang Sun[a]

[a] *School of Software, Tsinghua University, Beijing 100084, PR China*
[b] *Department of Computer Science and Technology, Tsinghua University, Beijing 100084, PR China*
[c] *Laboratory of Computational Physics, Institute of Applied Physics and Computational Mathematics, Beijing 100088, PR China*

Received 21 November 2006; received in revised form 17 August 2007

Abstract

Dynamic partial differential equation (PDE) parametric curves which can be expressed as a coupled system of two hyperbolic equations are developed. In curve design, dynamic PDE parametric curves can be modified intuitively and are more flexible than ordinary differential equation (ODE) curves. The calculation of dynamic PDE parametric curves must recur to numerical methods and a three-level finite difference scheme is proposed. Approximation and stability properties for the scheme are proved and convergence property is derived. An example of interpolating PDE curves is presented as an application of dynamic PDE parametric curves.

Keywords: PDE curves; Interpolation; Finite difference method; Convergence

1. Introduction

Bloor et al. [1] propose a method of representing surfaces as the solution of partial differential equations (PDEs). They define blending surfaces as the solutions of two-dimensional elliptic boundary-value problems. Usually, B-splines or NURBS curves are adopted as tools in a CAD system. To keep compatible with a NURBS system, Bloor et al. [2] also represent PDE surfaces in terms of B-splines. PDE surfaces have an emphasis on the functional surfaces. For example, they can be used to design the outline surface of an aircraft [3] or other complex surfaces [21]. Generally, the calculation of PDE surface recurs to numerical methods such as spectral approximation [4], B-splines approximation [5], etc. As mentioned in [5], PDE surfaces have the advantages such as natural fairness, and simplicity of constructing blending surfaces. Of course, they also have the disadvantage that the modification is inconvenient. Ugail et al. [17] propose techniques to modify the PDE surface by changing the boundary conditions.

Curve design is a basic part in a CAD system. When a surface is displayed with the wire frame model, it is also displayed as curve grids. Generally, curves such as lines, circles, etc. are adopted as simple geometric entities in CAD systems. These entities can be expressed as NURBS curves [11]. NURBS curves adopt piecewise polynomial or piecewise rational describing the geometry entities and have many advantages such as the representation form is simple, etc. However, many problems of engineering, geology and other fields require the smooth curves whose shapes cannot be described by such simple entities. For example, the shape of an aircraft requires hydrodynamic properties

* Corresponding author. School of Software, Tsinghua University, Beijing 100084, PR China.
E-mail address: xuzhengliu06@gmail.com (X.-Z. Liu).

and the curve described by differential equations may have priority. Li et al. [12,13] define the landing curve of a plane as a solution of ordinary differential equations (ODEs). With different constraints, curves can also be described as variational problems [9,18]. In 2003, Kouibia et al. [10] construct a curve from data constituted by some approximation points and an ODE problem.

Combining NURBS and Lagrangian dynamics, Qin et al. [15] propose D-NURBS curves. D-NURBS curves are more flexible than NURBS in curve design because they have more parameters. Using the similar idea, and basing on the finite difference (FD) method for elliptic boundary-value problem, Du et al. [5,6] propose dynamic PDE surfaces. The dynamic PDE surface is a discrete model and can be modified intuitively.

In this paper, dynamic PDE curves which can be expressed as a coupled system of two hyperbolic equations are proposed. From the view of intuition to design curves, points on both PDE and NURBS curves can be manipulated directly. But the continuity of NURBS curves at the breakpoints is decreased [11]. PDE curves have consistent continuity. Compared to ODE curves, dynamic PDE curves are more flexible in curve design and can be modified intuitively. The calculation of dynamic PDE curves must recur to numerical methods such as FD method [14,16,20,8,19], finite element (FE) method, etc. Here, we adopt the FD method to calculate dynamic PDE parametric curves and a three-level FD scheme is proposed.

The remaining part of the paper is structured as follows. In Section 2, dynamic PDE parametric curves are defined. A three-level FD scheme is proposed in Section 3. Both stability and approximation properties are also obtained. A numerical example illustrates the correctness of the theoretical analysis. In Section 4, interpolating PDE curves are presented as an application of dynamic PDE parametric curves. Finally, the conclusions are drawn in the last section.

2. Dynamic PDE parametric curves

In [10], an ODE curve $C(u)$ is defined as the solution of the following ODE:

$$\begin{aligned}
&\frac{\mathrm{d}^4 C(u)}{\mathrm{d}u^4} = f(u), \quad u \in [0,1],\\
&C(0) = C_0 = (x_0, y_0), \quad C(1) = C_1 = (x_1, y_1),\\
&\frac{\partial C}{\partial u}(0,t) = C_0' = (x_0', y_0'), \quad \frac{\partial C}{\partial u}(1,t) = C_1' = (x_1', y_1').
\end{aligned} \tag{1}$$

The ODE curve has both the interpolating and smoothness properties, and cannot be replaced by simple entities in some fields such as engineering field, geology field, etc. However, ODE curves have the disadvantage that they cannot be modified intuitively.

A one-dimensional continuous oscillation system can be modelled as the following equation [7]:

$$m(u)\frac{\partial^2 C(u,t)}{\partial t^2} + d(u)\frac{\partial C(u,t)}{\partial t} - \frac{\partial}{\partial u}\left(k(u)\frac{\partial C(u,t)}{\partial u}\right) = f(u,t), \tag{2}$$

where $C(u,t)$ is the current position, t is the time variable and $u \in [0,1]$ is the spatial variable. The coefficient functions $m(u), d(u), k(u)$ are related to mass, damping and stiffness, respectively. Here, the initial and boundary conditions are omitted.

Combining models (1) and (2), a dynamic PDE parametric curve can be defined as the solution of the following coupled system of two hyperbolic equations. Denote a planar dynamic PDE parametric curve as $C(u,t)=(x(u,t), y(u,t))$; then $C(u,t)$ satisfies

$$\begin{aligned}
&\frac{\partial^2 C(u,t)}{\partial t^2} + A(u,t,C)\frac{\partial C(u,t)}{\partial t} - \frac{\partial}{\partial u}\left(B(u,t,C)\frac{\partial C(u,t)}{\partial u}\right)\\
&\quad + \frac{\partial^2}{\partial u^2}\left(D(u,t,C)\frac{\partial^2 C(u,t)}{\partial u^2}\right) = F(u,t),
\end{aligned} \tag{3}$$

where $u \in [0,1]$, $t \in [0,T]$ are the spatial and the temporal variables, respectively. The coefficient functions $A(u,t) = (a_1(u,t,x(u,t)), a_2(u,t,y(u,t)))$, $B(u,t,C)=(b_1(u,t,x(u,t)), b_2(u,t,y(u,t)))$ and $D(u,t,C)=(d_1(u,t,x(u,t)),$

$d_2(u,t,y(u,t)))$ satisfy a Lipschitz continuous condition. Moreover, they all have a positive lower bound. The right-hand side function $F(u,t,C)=(f_1(u,t,x(u,t)),\ f_2(u,t,y(u,t)))$ is continuous. The initial–boundary values of model (3) are the following:

$$
\begin{aligned}
&C(u,t)|_{t=0} = C(u) = (x(u), y(u)), \quad u \in [0,1],\\
&\left.\frac{\partial C(u,t)}{\partial t}\right|_{t=0} = C_t(u) = (x_t(u), y_t(u)), \quad u \in [0,1],\\
&C(0,t) = C_0 = (x_0, y_0), \quad C(1,t) = C_1 = (x_1, y_1),\\
&\frac{\partial C}{\partial u}(0,t) = C_0' = (x_0', y_0'), \quad \frac{\partial C}{\partial u}(1,t) = C_1' = (x_1', y_1').
\end{aligned} \tag{4}
$$

Using discrete function techniques, Zhou [20] proved the existence and uniqueness of the solution of generic parabolic equations and wave equations. Applying the same techniques, the existence and uniqueness of the solution of system (3)–(4) can be obtained.

3. FD scheme and convergence

Dynamic PDE parametric curves can be expressed as a coupled system of two hyperbolic equations. The solution of the system can be equivalent to the solutions of two single hyperbolic equations because there is no dependence between the two variables. Here, we present an FD scheme for a single hyperbolic equation. For convenience to numerical analysis, we adopt the zero boundary value and the model problem can be rewritten as

$$
\begin{aligned}
&\frac{\partial^2 x(u,t)}{\partial t^2} + a(u,t,x)\frac{\partial x(u,t)}{\partial t} - \frac{\partial}{\partial u}\left(b(u,t,x)\frac{\partial x(u,t)}{\partial u}\right)\\
&\quad + \frac{\partial^2}{\partial u^2}\left(d(u,t,x)\frac{\partial^2 x(u,t)}{\partial u^2}\right) = f(u,t,x), \quad u \in [0,1], \quad t \in [0,T],\\
&x(u,0) = x_0(u), \quad x_t(u,0) = x_{t0}(u), \quad u \in [0,1],\\
&x(0,t) = 0, \quad x(1,t) = 0, \quad x_u(0,t) = 0, \quad x_u(1,t) = 0, \quad t \in [0,T].
\end{aligned} \tag{5}
$$

The coefficient functions $a(u,t,x), b(u,t,x), d(u,t,x)$ are Lipschitz continuous and have positive lower bound values a_*, b_*, d_*, respectively.

3.1. FD scheme

Divide the interval $[0,1]$ and $[0,T]$ into J, L small intervals. Denote $\Delta t = T/L, t_n = n\Delta t, h = 1/J, u_i = ih$. We introduce some notations: $\phi_t^n = \phi_t|_{t=t_n}$, $\phi_j^n(\psi) = \phi(u_j, t_n, \psi_j^n)$, $\phi_{j+1/2}^n(\psi) = \phi(u_{j+1/2}, t_n, \frac{1}{2}(\psi_{j+1}^n + \psi_j^n))$, $\bar{\phi}^n = \frac{1}{2}(\phi^{n+1} + \phi^{n-1})$, $d_t\phi^n = (\phi^{n+1} - \phi^n)/\Delta t$, $\partial_t\phi^n = (\phi^{n+1} - \phi^{n-1})/2\Delta t = \frac{1}{2}(d_t\phi^n + d_t\phi^{n-1})$, $\partial_{tt}\phi^n = (\phi^{n+1} - 2\phi^n + \phi^{n-1})/(\Delta t)^2 = (1/\Delta t)(d_t\phi^n - d_t\phi^{n-1})$, $\delta\phi_j = (\phi_{j+1} - \phi_j)/h$ and $\delta^2\phi_j = (\phi_{j+1} - 2\phi_j + \phi_{j-1})/h^2 = (\delta\phi_j - \delta\phi_{j-1})/h$. Let K be a generic positive constant and ε be a small positive constant. The discrete norms are defined as follows:

$$
\|\phi\| = \left(\sum_{j=0}^{J} |\phi_j|^2 h\right)^{1/2}, \quad \|\delta\phi\| = \left(\sum_{j=0}^{J-1} |\delta\phi_j|^2 h\right)^{1/2},
$$

$$
\|\delta^2\phi\| = \left(\sum_{j=1}^{J-1} |\delta^2\phi_j|^2 h\right)^{1/2}, \quad \|\phi\|_\infty = \max_{0 \leqslant j \leqslant J} |\phi_j|.
$$

If $\phi_0=\phi_1=\phi_{J-1}=\phi_J=0$ (namely, $\delta\phi_0=\delta\phi_{J-1}=0$), we have the following equalities:

$$\|\phi\|=\left(\sum_{j=2}^{J-2}|\phi_j|^2h\right)^{1/2},\quad \|\delta\phi\|=\left(\sum_{j=1}^{J-2}|\delta\phi_j|^2h\right)^{1/2},$$
$$\|\phi\|_\infty=\max_{1\leqslant j\leqslant J-1}|\phi_j|.$$

Denote X as the approximation of the solutions x and the FD solution of (5) is given by finding X_j^{n+1} such that

$$\begin{aligned}&\partial_{tt}X_j^n+a_j^n(X)\partial_tX_j^n-\frac{1}{h}\left[b_{j+1/2}^n(X)\delta\bar{X}_j^n-b_{j-1/2}^n(X)\delta\bar{X}_{j-1}^n\right]\\&\quad+\frac{1}{h^2}\left[d_{j+1}^n(X)\delta^2\bar{X}_{j+1}^n-2d_j^n(X)\delta^2\bar{X}_j^n+d_{j-1}^n(X)\delta^2\bar{X}_{j-1}^n\right]=f_j^n(X),\end{aligned}\tag{6}$$

where $j=1,\dots,J-1$, $n=1,2,\dots$, $a_j^n(X)=a(u_j,t_n,X^n)$, $b_{j+1/2}^n(X)=b(u_{j+1/2},t_n,\frac{1}{2}(X_{j+1}^n+X_j^n))$, $d_j^n(X)=d(u_j,t_n,X^n)$ and $f_j^n(X)=f(u_j,t_n,X^n)$. The boundary and initial values are $X_0^n=X_J^n=X_1^n=X_{J-1}^n=0$ and $X_j^0=x_0(u_j)$, $(X_j^1-X_j^0)/\Delta t=x_{t0}(u_j)+(\Delta t/2)x_{tt0}(u_j)$, where $x_{tt0}(u)=f(u,0,x_0(u))-a(u,0,x_0(u))x_{t0}(u)+\frac{\partial}{\partial u}(b(u,0,x_0(u))\partial x_0(u)/\partial u)-(\partial^2/\partial u^2)(d(u,0,x_0(u))\partial^2x_0(u)/\partial u^2)$. The FD scheme (6) is a three-level scheme.

3.2. Convergence

Denote the truncation error as

$$\begin{aligned}R_j^n=&\,\partial_{tt}x_j^n+a_j^n(x)\partial_tx_j^n-\frac{1}{h}\left[b_{j+1/2}^n(x)\delta\bar{x}_j^n-b_{j-1/2}^n(x)\delta\bar{x}_{j-1}^n\right]\\&+\frac{1}{h^2}\left[d_{j+1}^n(x)\delta^2\bar{x}_{j+1}^n-2d_j^n(x)\delta^2\bar{x}_j^n+d_{j-1}^n(x)\delta^2\bar{x}_{j-1}^n\right]-f_j^n(x).\end{aligned}$$

Now, we have $R_j^n=\mathrm{O}(h^2+(\Delta t)^2)$. Denoting $\xi_j^n=X_j^n-x_j^n$, and subtracting (5) from (6), we get the error equation:

$$\begin{aligned}&\partial_{tt}\xi_j^n+a_j^n(X)\partial_t\xi_j^n-\frac{1}{h}\left[b_{j+1/2}^n(X)\delta\bar{\xi}_j^n-b_{j-1/2}^n(X)\delta\bar{\xi}_{j-1}^n\right]\\&\quad+\frac{1}{h^2}\left[d_{j+1}^n(X)\delta^2\bar{\xi}_{j+1}^n-2d_j^n(X)\delta^2\bar{\xi}_j^n+d_{j-1}^n(X)\delta^2\bar{\xi}_{j-1}^n\right]\\&\quad=\frac{1}{h}\left\{[b_{j+1/2}^n(X)-b_{j+1/2}^n(x)]\delta\bar{x}_j^n-[b_{j-1/2}^n(X)-b_{j-1/2}^n(x)]\delta\bar{x}_{j-1}^n\right\}\\&\qquad-\frac{1}{h^2}\left\{[d_{j+1}^n(X)-d_{j+1}^n(x)]\delta^2\bar{x}_{j+1}^n-2[d_j^n(X)-d_j^n(x)]\delta^2\bar{x}_j^n+[d_{j-1}^n(X)-d_{j-1}^n(x)]\delta^2\bar{x}_{j-1}^n\right\}\\&\qquad-\left[a_j^n(X)-a_j^n(x)\right]\partial_tx_j^n+\left[f_j^n(X)-f_j^n(x)-R_j^n\right].\end{aligned}\tag{7}$$

Let the test function be $\partial_t\xi_j^n$ and do discrete inner product with error equation (7), multiply with $h\Delta t$, and sum for $j=2,3,\dots,J-2$ and $n=1,2,\dots,N-1$. Using Grownwall's Lemma [8], discrete Sobolev inequality and deductive reasoning, we obtain the following theorem.

Theorem 1. *If the following equality holds*:

$$\|\xi^0\|^2+\|d_t\xi^0\|^2+\|\delta\xi^0\|^2+\|\delta^2\xi^0\|^2+\|\xi^1\|^2+\|\delta\xi^1\|^2+\|\delta^2\xi^1\|^2=\mathrm{O}(h^2+(\Delta t)^2),$$

then the FD scheme (6) *has the following approximation property*:

$$\begin{aligned}&\|d_t\xi^{N-1}\|^2+\sum_{n=1}^{N-1}\|\partial_t\xi^n\|^2\Delta t+\|\xi^N\|^2+\|\xi^{N-1}\|^2\\&\quad+\|\delta\xi^N\|^2+\|\delta\xi^{N-1}\|^2+\|\delta^2\xi^N\|^2+\|\delta^2\xi^{N-1}\|^2\leqslant K(h^2+(\Delta t)^2).\end{aligned}\tag{8}$$

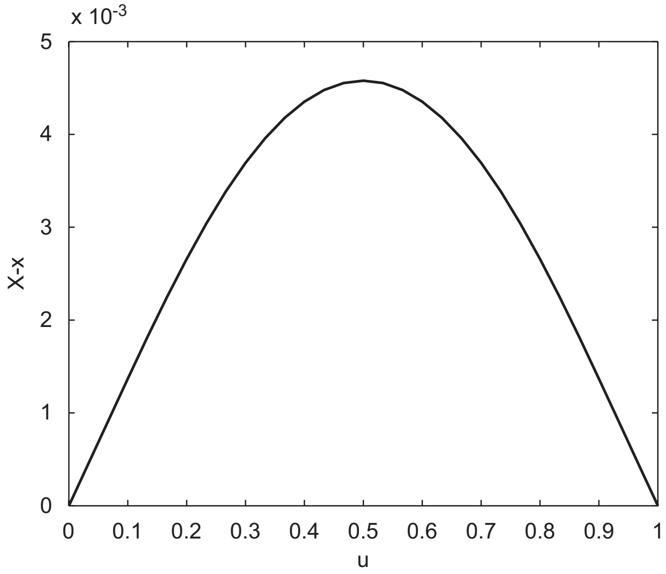

Fig. 1. The error between the numerical solution and the exact solution at the time $t = 15$ s.

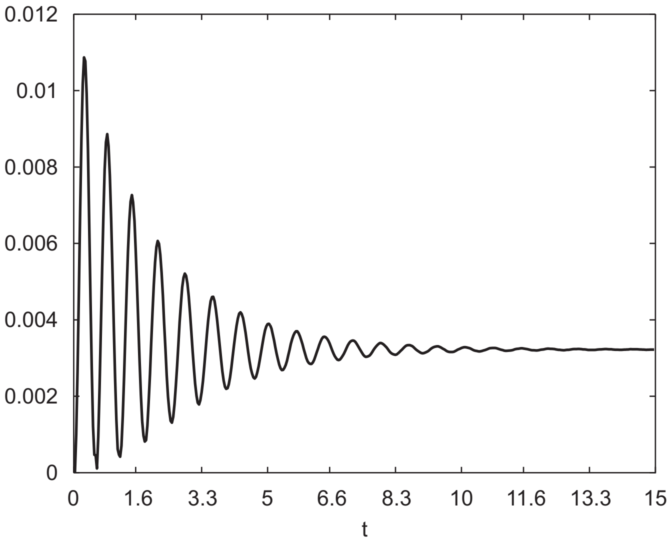

Fig. 2. The variation of a discrete L^2 norm for $X - x$.

Proof. See the Appendix.

Let the test function be $\partial_t X_j^n$. With the deduction analogous to that of (8), we can obtain the following stability result.

Theorem 2. *Under the same assumption as in Theorem* 1, *the FD scheme* (6) *has the following stability property*:

$$\|d_t X^{N-1}\|^2 + \sum_{n=1}^{N-1} \|\partial_t X^n\|^2 \Delta t + \|\delta X^N\|^2 + \|\delta X^{N-1}\|^2 + \|\delta^2 X^N\|^2 + \|\delta^2 X^{N-1}\|^2$$

$$\leqslant K(\|d_t X^0\|^2 + \|\delta X^0\|^2 + \|\delta^2 X^0\| + \|\delta X^1\|^2 + \|\delta^2 X^1\|^2) + K \sum_{n=1}^{N-1} \|f^n(X)\|^2 \Delta t. \tag{9}$$

From Theorems 1 and 2, we see that the FD scheme (6) is convergent with a rate $O(h^2 + (\Delta t)^2)$. Since we do not need any additional condition between h and Δt during the deductions of Theorems 1 and 2, scheme (6) is unconditionally stable.

If the coefficient functions $a(u,t,x), b(u,t,x), d(u,t,x)$ of (5) equal zero ($b(u,t,x), d(u,t,x)$ cannot be zero at the same time), the model problem will be simplified and the properties will still hold. Take (8) as an example. If $a(u,t,x) \equiv 0$, $b(u,t,x) \equiv 0$ or $d(u,t,x) \equiv 0$, the items $\sum_{n=1}^{N-1} \|\partial_t \xi^n\|^2 \Delta t$, $\|\delta X^N\|^2 + \|\delta X^{N-1}\|^2$ or $\|\delta^2 X^N\|^2 + \|\delta^2 X^{N-1}\|^2$ on the left-hand side of (8) will disappear.

3.3. Numerical experiment

Let the coefficient function of (5) be

$$
\begin{aligned}
&a(u,t,x) = 1.0, \quad b(u,t,x) = 0.5x(u,t), \quad d(u,t,x) = x(u,t),\\
&f(u,t,x) = (1 + e^{-t})^2(\sin^2(\pi u) - \cos^2(\pi u))(2\pi^4 + 0.5\pi^2)
\end{aligned}
$$

and let the initial–boundary values be given by

$$
\begin{aligned}
&x|_{t=0} = 2\sin(\pi u), \quad x_t|_{t=0} = -\sin(\pi u),\\
&x|_{u=0} = 0, \quad x|_{u=1} = 0,\\
&x_u|_{u=0} = \pi(1 + e^{-t}), \quad x_u|_{u=1} = -\pi(1 + e^{-t}).
\end{aligned}
$$

Then the exact solution of the hyperbolic equation is

$$
x(u,t) = (1 + e^{-t}) \sin(\pi u).
$$

Let $T = 15$ s, divide the spatial and the temporal interval into $J = 30$, $L = 450$ small equal intervals, and we have $\Delta t = h = \frac{1}{30}$, $h^2 + (\Delta t)^2 \approx 0.0022$. Use the FD scheme (6), and we can obtain the numerical solution. Fig. 1 presents the error of $X - x$ at $t = 15$ s. Fig. 2 illustrates the variation of a discrete L^2 norm. From Fig. 2, we can conclude that the discrete L^2 norm of $X - x$ is $O(h^2 + (\Delta t)^2)$. The numerical example verifies the error analysis above.

4. Applications

In curve design, the information of the two end points can be easily determined. The internal points can be placed approximately. Then an interpolating curve can be constructed by a certain method. If a polynomial function is adopted, on the one hand, the degree of the polynomial function may be high. On the other hand, there may exist the so-called Runge phenomenon. A piecewise polynomial may satisfy the interpolation conditions easily, but the smoothness on the node decreases and the smoothness property is necessary for some cases. The ODE curves proposed in [9] can provide this smoothness property. However, the ODE curves are difficult to be modified intuitively. Dynamic PDE parametric curves can be modified intuitively except the interpolation and smoothness property. Dynamic PDE parametric curves possess many degrees of freedom including the coefficient functions $A(u,t)$, $B(u,t)$, $D(u,t)$, $F(u,t)$ and initial conditions. These functions have practical physical meaning. For example, $A(u,t)$ is related to the dampness of a PDE curve. $B(u,t)$ represents the transmitting velocity of the curve. $D(u,t)$ represents the ability to resist the bending of the curve. The right-hand side function $F(u,t)$ means the external force to the curve.

PDE curves can be modified by revising the coefficient functions or initial conditions. But these modifications are nonintuitive and difficult to apply to interactive design. Dynamic PDE parametric curves can be modified intuitively by revising the right-hand side function. By defining the right-hand side function of a PDE curve, we can define the attracting force of a point to the PDE curve and the force can attract the curve passing through the point. Denote the PDE curve as $C(u,t)$ and the point as p. Then, the force can be defined as follows:

$$
f(p) = \int k(p - C(u,t))\delta(u - u_p)\,du = k(p - C(u_p,t)), \tag{10}
$$

where $u_p \in [0,1]$ represents the parameter of the point on the PDE curve that is closest to p. k is a constant. Because of the smoothness requirement of the right-hand side function, we use the following smooth function $g(u,u_p,\varepsilon)$ to

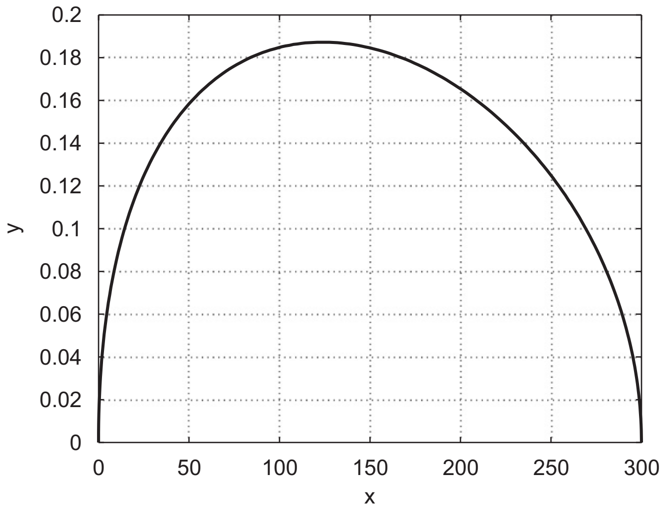

Fig. 3. The initial dynamic PDE parametric curve.

avoid the singularity of the delta function:

$$g(u,u_p,\varepsilon)=\begin{cases}0, & u\in[0,u_p-\varepsilon),\\ \dfrac{9}{2}\left(\dfrac{u-u_p+\varepsilon}{\varepsilon}\right)^3, & u\in\left[u_p-\varepsilon,u_p-\dfrac{2}{3}\varepsilon\right),\\ \dfrac{9}{2}\left[\left(\dfrac{u-u_p+\varepsilon}{\varepsilon}\right)^3-3\left(\dfrac{u-u_p+\varepsilon}{\varepsilon}-\dfrac{1}{3}\right)^3\right], & u\in\left[u_p-\dfrac{2}{3}\varepsilon,u_p-\dfrac{1}{3}\varepsilon\right),\\ 1+\dfrac{9}{2}\left(\dfrac{u-u_p}{\varepsilon}\right)^3, & u\in\left[u_p-\dfrac{1}{3}\varepsilon,u_p\right),\\ 1-\dfrac{9}{2}\left(\dfrac{u-u_p}{\varepsilon}\right)^3, & u\in\left[u_p,u_p+\dfrac{1}{3}\varepsilon\right),\\ -\dfrac{9}{2}\left[\left(\dfrac{u-u_p-\varepsilon}{\varepsilon}\right)^3-3\left(\dfrac{u-u_p-\varepsilon}{\varepsilon}+\dfrac{1}{3}\right)^3\right], & u\in\left[u_p+\dfrac{1}{3}\varepsilon,u_p+\dfrac{2}{3}\varepsilon\right),\\ -\dfrac{9}{2}\left(\dfrac{u-u_p-\varepsilon}{\varepsilon}\right)^3, & u\in\left[u_p+\dfrac{2}{3}\varepsilon,u_p+\varepsilon\right),\\ 0, & u\in[u_p+\varepsilon,1],\end{cases}$$

where ε is a small positive constant and 2ε represents the width in parametric domain affected by the point p. The function $g(u,u_p,\varepsilon)$ is symmetrical around $u=u_p$ on [0, 1] and its second derivative is continuous. The right-hand side function of (10) can be replaced by $f(p)=k(p-C(u_p,t))g(u,u_p,\varepsilon)$.

This idea can be used directly to solve the dynamic PDE interpolation problem with the two end points p_0, p_n, tangent vectors p_0', p_n' and the point set $P=\{p_1,p_2,\ldots,p_{n-1}\}$. To construct a PDE curve satisfying these interpolation conditions, firstly the initial curve of the PDE curve can be constructed by Hermite method using the end points information. Secondly, the right-hand side function can be defined as $F(u,t)=\sum_{i=1}^{n}f(p_i)=k\sum_{i=1}^{n}(p_i-C(u_i,t))g(u,u_i,\varepsilon)$. Finally, the interpolating PDE curve can be calculated using the FD scheme (6).

Consider the interpolating data

$$p_0=(0,0),\quad p_0'=(28.0,65.0),\quad p_4=(300.0,0.0),\quad p_4'=(55.0,-37.0),$$
$$P=\{p_1=(100.0,60.0),\ p_2=(150.0,70.0),\ p_3=(200.0,60.0)\}.$$

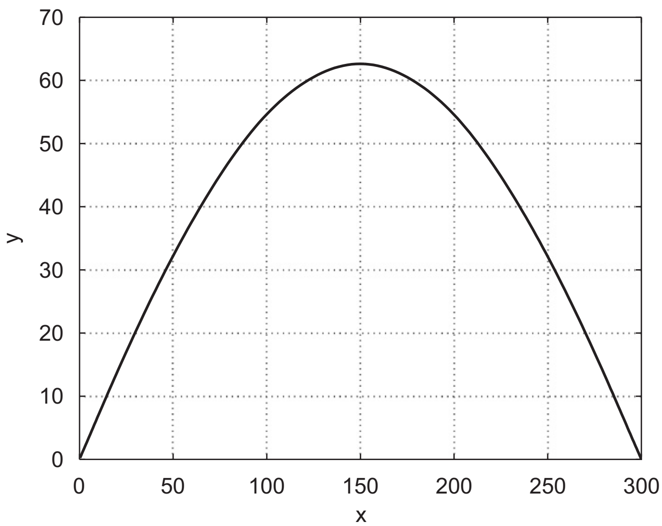

Fig. 4. The intermediate dynamic PDE parametric curve.

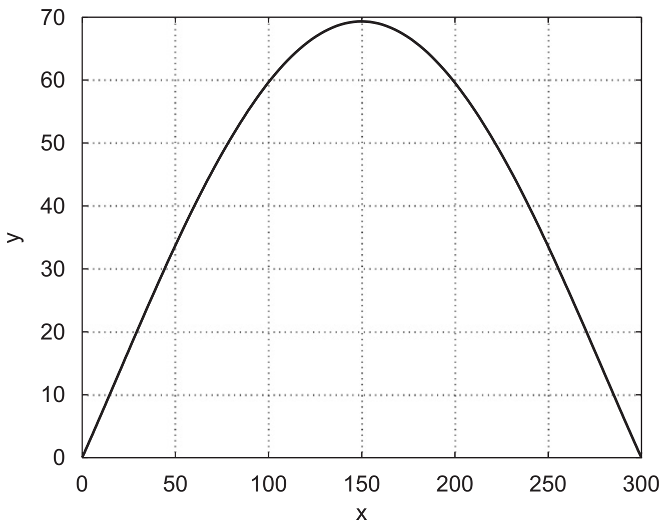

Fig. 5. The final dynamic PDE parametric curve.

Let the coefficient functions of PDE curve be constants $A = (0.0, 0.0)$ $B = (0.0, 0.0)$ and $D = (0.01, 0.01)$. Let the constant $k = 500.0$ and $\varepsilon = 0.01$. The initial curve $C_0(u)$ can be constructed by Hermite method using the end points p_0, p_4 and their tangent vectors p_0', p_4'. Let $C_t(u) \equiv (0.0, 0.0)$, namely the initial velocity of the initial curve is zero. Fig. 3 is a plot of the initial curve. The initial curve only interpolates the end points p_0, p_4 and the end tangents p_0', p_4'. It does not interpolate the points p_1, p_2, p_3. Using the initial curve, we can get the intermediate curve after several iterations. The intermediate curve does not pass through the three points p_1, p_2, p_3, but it has the tendency to interpolate them. Fig. 4 is an intermediate dynamic PDE parametric curve. When the dynamic PDE curve reaches its stable status, we obtain the final curve which interpolates both the points p_0, p_1, p_2, p_3, p_4 and the end tangents p_0', p_4' (Fig. 5). We can also see the end tangent of the final curve after zooming the plot around the point p_4 (Fig. 6).

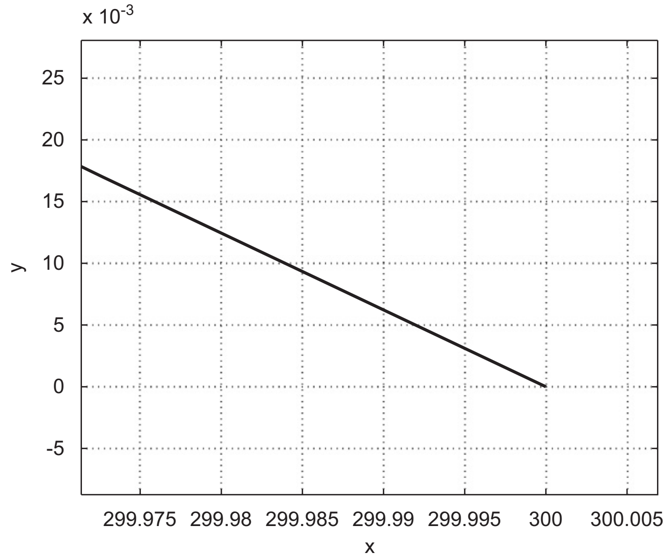

Fig. 6. The zoom of Fig. 5 around the point p_4.

5. Conclusions

The parametric PDE curve has a natural fairness and good physical background. It can be modified intuitively in curve design and has more degrees of freedom than ODE curves. A three-level FD scheme is proposed for calculating dynamic PDE parametric curves and the approximation and stability properties are obtained.

This idea can be applied to surface directly, and the surface can be expressed as a two-dimensional coupled system of two hyperbolic equations. Besides the FD scheme to calculate the PDE parametric curves, FE schemes for dynamic PDE parametric curves can be considered. This will be the topic of future research.

Acknowledgment

This research is supported by the Chinese 973 Program (2004CB719400) and the National Natural Science Foundation of China (60403047, 60533070). The second author is supported by the National Natural Science Foundation of China (Nos. 10501004, 10471011, 10431050), the Foundation of CAEP (20040653, 2003Z0603) and the Foundation of LCP IAPCM.

Appendix A. The proof of Theorem 1

Before deriving the approximation properties of (6), some equations or inequalities are presented.
If $\psi_1 = \psi_{J-1} = 0$, we have

$$\sum_{j=2}^{J-2} (\delta\phi_{j-1}, \psi_j) = -\sum_{j=1}^{J-2} (\phi_j, \delta\psi_j). \tag{A.1}$$

If $\psi_0 = \psi_1 = \psi_{J-1} = \psi_J = 0$, we get

$$\sum_{j=2}^{J-2} (\delta^2\phi_j, \psi_j) = \sum_{j=1}^{J-1} (\phi_j, \delta^2\psi_j). \tag{A.2}$$

Denoting $\Phi=\Phi(\Psi)$ as a smooth function with enough continuity, the following inequality:

$$|\Phi(\phi^n)-\Phi(\psi^n)|\leqslant K|\phi^n-\psi^n|$$

holds. Let $\Phi=b(u,t,x)$, $\phi=\frac{1}{2}(X_{j+1}+X_j)$, $\psi=\frac{1}{2}(x_{j+1}+x_j)$, $j=1,2,\ldots,J-2$, respectively, we obtain the following estimates:

$$|b^n_{j+1/2}(X)-b^n_{j+1/2}(x)|\leqslant K(|\xi^n_{j+1}|+|\xi^n_j|). \tag{A.3}$$

Similarly, let $\Phi=d(u,,t,x)$, $\phi=X_j$, $\psi=x_j$, $j=1,2,\ldots,J-2$, we get

$$|d^n_j(X)-d^n_j(x)|\leqslant K|X^n_j-x^n_j|=K|\xi^n_j|. \tag{A.4}$$

For a smooth function Φ, the inequality

$$\begin{aligned}&|\Phi(\phi^n)-\Phi(\psi^n)-[\Phi(\phi^{n+1})-\Phi(\psi^{n+1})]|\\&\quad\leqslant K\Delta t[|d_t(\phi^n-\psi^n)|+(|d_t(\phi^n-\psi^n)|+|d_t\psi^n|)|\phi^n-\psi^n|]\end{aligned}$$

holds. Let $\Phi=b(u,t,x)$, $\phi=\frac{1}{2}(X_{j+1}+X_j)$, $\psi=\frac{1}{2}(x_{j+1}+x_j)$, $j=1,2,\ldots,J-2$, we obtain the estimates

$$\begin{aligned}&|[b^n_{j+1/2}(X)-b^n_{j+1/2}(x)]-[b(u_{j+1/2},t_n,\tfrac{1}{2}(X^{n+1}_{j+1}+X^{n+1}_j))-b(u_{j+1/2},t_n,\tfrac{1}{2}(x^{n+1}_{j+1}+x^{n+1}_j))]|\\&\quad\leqslant K\Delta t[|d_t\xi^n_{j+1}|+|d_t\xi^n_j|+(\|d_t\xi^n\|_\infty+1)(|\xi^n_{j+1}|+|\xi^n_j|)].\end{aligned} \tag{A.5}$$

Similarly, let $\Phi=d(u,t,x)$, $\phi=X_j$, $\psi=x_j$, $j=1,2,\ldots,J-1$, and we have

$$\begin{aligned}&|[d^n_j(X)-d^n_j(x)]-[d(u_j,t_n,X^{n+1}_j)-d(u_j,t_n,x^{n+1}_j)]|\\&\quad\leqslant K\Delta t[|d_t\xi^n_j|+(\|d_t\xi^n\|_\infty+1)|\xi^n_j|].\end{aligned} \tag{A.6}$$

For the smooth function $\Phi=\Phi(t,\Psi)$, we have the inequality

$$|\Phi(t_{n+1},\phi^{n+1})-\Phi(t_{n+1},\psi^{n+1})-[\Phi(t_n,\phi^{n+1})-\Phi(t_n,\psi^{n+1})]|\leqslant K\Delta t|\phi^{n+1}-\psi^{n+1}|.$$

Let $\Phi=b(u,t,x)$, $\phi=\frac{1}{2}(X_{j+1}+X_j)$, $\psi=\frac{1}{2}(x_{j+1}+x_j)$, $j=1,2,\ldots,J-2$, the following inequality stands:

$$\begin{aligned}&|[b^{n+1}_{j+1/2}(X)-b^{n+1}_{j+1/2}(x)]-[b(u_{j+1/2},t_n,\tfrac{1}{2}(X^{n+1}_{j+1}+X^{n+1}_j))\\&\quad-b(u_{j+1/2},t_n,\tfrac{1}{2}(x^{n+1}_{j+1}+x^{n+1}_j))]|\leqslant K\Delta t(|\xi^{n+1}_{j+1}|+|\xi^{n+1}_j|).\end{aligned} \tag{A.7}$$

Similarly, let $\Phi=d(u,t,x)$, $\phi=X_j$, $\psi=x_j$, $j=1,2,\ldots,J-1$, we get

$$\begin{aligned}&|[d^{n+1}_j(X)-d^{n+1}_j(x)]-[d(u_j,t_n,X^{n+1}_j)-d(u_j,t_n,x^{n+1}_j)]|\\&\quad\leqslant K\Delta t|X^{n+1}_j-x^{n+1}_j|\leqslant K\Delta t|\xi^{n+1}_j|.\end{aligned} \tag{A.8}$$

For $j=1,2,\ldots,J-2$, combining (A.5) with (A.7), we get

$$\begin{aligned}&|[b^n_{j+1/2}(X)-b^n_{j+1/2}(x)]-[b^{n+1}_{j+1/2}(X)-b^{n+1}_{j+1/2}(x)]|\\&\quad\leqslant K\Delta t[|d_t\xi^n_{j+1}|+|d_t\xi^n_j|+|\xi^{n+1}_{j+1}|+|\xi^{n+1}_j|+(\|d_t\xi^n\|_\infty+1)(|\xi^n_{j+1}|+|\xi^n_j|)].\end{aligned} \tag{A.9}$$

Combining (A.6) with (A.8), we have

$$|[d^n_j(X)-d^n_j(x)]-[d^{n+1}_j(X)-d^{n+1}_j(x)]|\leqslant K\Delta t[|d_t\xi^n_j|+|\xi^{n+1}_j|+(\|d_t\xi^n\|_\infty+1)|\xi^n_j|]. \tag{A.10}$$

Next, we derive the approximation properties of the FD scheme (6). Let the test function be $\partial_t \xi_j^n$ and do discrete inner product with error equation (7), multiply with $h\Delta t$, and sum for $j = 2, 3, \ldots, J-2$ and $n = 1, 2, \ldots, N-1$:

$$\sum_{n=1}^{N-1}\sum_{j=2}^{J-2}(\partial_{tt}\xi_j^n, \partial_t \xi_j^n)h\Delta t = \frac{1}{2}[\|d_t\xi^{N-1}\|^2 - \|d_t\xi^0\|^2], \tag{A.11}$$

$$\sum_{n=1}^{N-1}\sum_{j=2}^{J-2}(a_j^n(X)\partial_t \xi_j^n, \partial_t \xi_j^n)h\Delta t \geqslant a_* \sum_{n=1}^{N-1}\|\partial_t \xi^n\|^2\Delta t. \tag{A.12}$$

Noting (A.1), we have

$$\begin{aligned}
&-\sum_{n=1}^{N-1}\sum_{j=2}^{J-2}\left(\frac{1}{h}[b_{j+1/2}^n(X)\delta\bar{\xi}_j^n - b_{j-1/2}^n(X)\delta\bar{\xi}_{j-1}^n], \partial_t\xi_j^n\right)h\Delta t\\
&\quad\geqslant \frac{b_*}{4}(\|\delta\xi^N\|^2 + \|\delta\xi^{N-1}\|^2) - K(\|\delta\xi^1\|^2 + \|\delta\xi^0\|^2) - K\Delta t\sum_{n=2}^{N-1}(1+\|\partial_t\xi^{n-1}\|_\infty)\|\delta\xi^{n-1}\|^2.
\end{aligned} \tag{A.13}$$

If $N = 2$, the last item on the right-hand side of (A.13) disappears and the inequality can be rewritten as

$$\begin{aligned}
&-\sum_{n=1}^{N-1}\sum_{j=2}^{J-2}\left(\frac{1}{h}[b_{j+1/2}^n(X)\delta\bar{\xi}_j^n - b_{j-1/2}^n(X)\delta\bar{\xi}_{j-1}^n], \partial_t\xi_j^n\right)h\Delta t\\
&\quad\geqslant \frac{b_*}{4}(\|\delta\xi^2\|^2 + \|\delta\xi^1\|^2) - K(\|\delta\xi^1\|^2 + \|\delta\xi^0\|^2).
\end{aligned}$$

Applying (A.2), we obtain

$$\begin{aligned}
&\sum_{n=1}^{N-1}\sum_{j=2}^{J-2}\left(\frac{1}{h^2}[d_{j+1}^n(X)\delta^2\bar{\xi}_{j+1}^n - 2d_j^n(X)\delta^2\bar{\xi}_j^n + d_{j-1}^n(X)\delta^2\bar{\xi}_{j-1}^n], \partial_t\xi_j^n\right)h\Delta t\\
&\quad\geqslant \frac{d_*}{4}(\|\delta^2\xi^N\|^2 + \|\delta^2\xi^{N-1}\|^2) - K(\|\delta^2\xi^1\|^2 + \|\delta^2\xi^0\|^2)\\
&\qquad - K\Delta t\sum_{n=2}^{N-1}(1+\|\partial_t\xi^{n-1}\|_\infty)\|\delta^2\xi^{n-1}\|^2.
\end{aligned} \tag{A.14}$$

Similar to (A.13), the last item on the right-hand side of (A.14) disappears if $N = 2$.

Combining (A.1), (A.3) and (A.9) we obtain

$$\begin{aligned}
&\sum_{n=1}^{N-1}\sum_{j=2}^{J-2}\left(\frac{1}{h}\{[b_{j+1/2}^n(X) - b_{j+1/2}^n(x)]\delta\bar{x}_j^n - [b_{j-1/2}^n(X) - b_{j-1/2}^n(x)]\delta\bar{x}_{j-1}^n\}, \partial_t\xi_j^n\right)h\Delta t\\
&\quad\leqslant K\Delta t\sum_{n=1}^{N-2}\|d_t\xi^n\|^2 + K\Delta t\sum_{n=2}^{N-1}\|\xi^n\|^2 + K\Delta t\sum_{n=1}^{N-2}(\|d_t\xi^n\|_\infty + 1)\|\xi^n\|^2 + K\Delta t\sum_{n=1}^{N-1}\|\delta\xi^n\|^2\\
&\qquad + K\|\xi^{N-1}\|^2 + \varepsilon(\|\delta\xi^N\|^2 + \|\delta\xi^{N-1}\|^2) + K(\|\xi^1\|^2 + \|\delta\xi^1\|^2 + \|\delta\xi^0\|^2).
\end{aligned} \tag{A.15}$$

Combining (A.2), (A.4) and (A.10), we have

$$
\begin{aligned}
&-\sum_{n=1}^{N-1}\sum_{j=2}^{J-2}\left(\frac{1}{h^2}\{[d_{j+1}^n(X)-d_{j+1}^n(x)]\delta^2\bar{x}_{j+1}^n-2[d_j^n(X)-d_j^n(x)]\delta^2\bar{x}_j^n\right.\\
&\left.+[d_{j-1}^n(X)-d_{j-1}^n(x)]\delta^2\bar{x}_{j-1}^n\},\partial_t\xi_j^n\right)h\Delta t\\
&\quad\leqslant K\Delta t\sum_{n=1}^{N-2}\|d_t\xi^n\|^2+K\Delta t\sum_{n=2}^{N-1}\|\xi^n\|^2+K\Delta t\sum_{n=1}^{N-2}(\|d_t\xi^n\|_\infty+1)\|\xi^n\|^2\\
&\qquad+K\Delta t\sum_{n=1}^{N-1}\|\delta^2\xi^n\|^2+K\|\xi^{N-1}\|^2+\varepsilon(\|\delta^2\xi^N\|^2+\|\delta^2\xi^{N-1}\|^2)\\
&\qquad+K(\|\xi^1\|^2+\|\delta^2\xi^1\|^2+\|\delta^2\xi^0\|^2).
\end{aligned}\tag{A.16}
$$

Noting $|a_j^n(X)-a_j^n(x)|\leqslant K|X_j^n-x_j^n|=K|\xi_j^n|$, we have

$$
\sum_{n=1}^{N-1}\sum_{j=2}^{J-2}([a_j^n(X)-a_j^n(x)]\partial_t x_j^n,\partial_t\xi_j^n)h\Delta t\leqslant K\sum_{n=1}^{N-1}\|\xi^n\|^2\Delta t+\varepsilon\sum_{n=1}^{N-1}\|\partial_t\xi^n\|^2\Delta t.\tag{A.17}
$$

The last item on the right-hand side of (7) has the following estimate:

$$
-\sum_{n=1}^{N-1}\sum_{j=2}^{J-2}(f_j^n(X)-f_j^n(x)-R_j^n,\partial_t\xi_j^n)h\Delta t\leqslant K\sum_{n=1}^{N-1}(\|\xi^n\|^2+\|R^n\|^2)\Delta t+\varepsilon\sum_{n=1}^{N-1}\|\partial_t\xi^n\|^2\Delta t.\tag{A.18}
$$

Summarizing (A.11)–(A.18), normalizing the coefficient on the left-hand side and combining the following inequality:

$$
\|\xi^n\|^2\leqslant\|\xi^0\|^2+\alpha\Delta t\sum_{l=0}^{n-1}\|d_t\xi^l\|^2+\frac{K}{\alpha}\Delta t\sum_{l=0}^{n}\|\xi^l\|^2,
$$

we obtain

$$
\begin{aligned}
&\|d_t\xi^{N-1}\|^2+\sum_{n=1}^{N-1}\|\partial_t\xi^n\|^2\Delta t+\|\xi^N\|^2+\|\xi^{N-1}\|^2+\|\delta\xi^N\|^2+\|\delta\xi^{N-1}\|^2+\|\delta^2\xi^N\|^2+\|\delta^2\xi^{N-1}\|^2\\
&\quad\leqslant K(\|\xi^0\|^2+\|d_t\xi^0\|^2+\|\delta\xi^0\|^2+\|\delta^2\xi^0\|^2+\|\xi^1\|^2+\|\delta\xi^1\|^2+\|\delta^2\xi^1\|^2)+K\sum_{n=1}^{N-1}\|R^n\|^2\Delta t\\
&\quad+K\Delta t\sum_{n=1}^{N-2}\|d_t\xi^n\|^2+K\Delta t\sum_{n=1}^{N-2}(1+\|d_t\xi^n\|_\infty)\|\xi^n\|^2\\
&\quad+K\Delta t\sum_{n=2}^{N-1}(1+\|d_t\xi^{n-2}\|_\infty+\|d_t\xi^{n-1}\|_\infty)(\|\delta\xi^{n-1}\|^2+\|\delta^2\xi^{n-1}\|^2).
\end{aligned}\tag{A.19}
$$

If $N=2$, the last item on the right-hand side of (A.19) will disappear. From Grownwall's Lemma [8], discrete Sobolev inequality and deductive reasoning, Theorem 1 is proved.

References

[1] M.I.G. Bloor, M.J. Wilson, Generating blend surfaces using partial differential equations, Comput.-Aided Design 21 (3) (1989) 165–171.
[2] M.I.G. Bloor, M.J. Wilson, Representing PDE surfaces in terms of B-splines, Comput.-Aided Design 22 (6) (1990) 324–331.

[3] M.I.G. Bloor, M.J. Wilson, Efficient parametrization of generic aircraft geometry, J. Aircraft 32 (6) (1995) 1269–1275.
[4] M.I.G. Bloor, M.J. Wilson, Spectral approximations to PDE surfaces, Comput.-Aided Design 28 (2) (1996) 145–152.
[5] H.X. Du, H. Qin, Dynamic PDE surfaces with flexible and general constraints, in: B. Barsky, Y. Shinagawa, and W. Wang, (eds.), Proceedings of the Pacific Graphics 2000, IEEE Computer Society, Hong Kong, 2000, pp. 213–222.
[6] H.X. Du, H. Qin, Dynamic PDE-based surface design using geometric and physical constraints, Graphical Models 67 (1) (2005) 43–71.
[7] T. Fang, P. Xue, The Theory and Applications of Oscillation, North-Western Polytechnical University Press, Xi'an, 1998.
[8] B. Gustafsson, H.O. Kreiss, J. Oliger, Time Dependent Problems and Difference Methods, Wiley-Interscience, New York, 1995.
[9] A. Kouibia, M. Pasadas, Smoothing variational splines, Appl. Math. Lett. 13 (2) (2000) 366–379.
[10] A. Kouibia, M. Pasadas, M.L. Rodriguez, Construction of ODE curves, Numer. Algorithms 34 (2–4) (2003) 367–377.
[11] P. Les, W. Tiller, The NURBS Book, 1997.
[12] Z.C. Li, Blending curves for landing problems by numerical differential equations, I. Mathematical modelling. Math. Comput. Modelling 31 (2–3) (2000) 161–177.
[13] Z.C. Li, H.T. Huang, Blending curves for landing problems by numerical differential equations, II. Numerical methods. Int. J. Comput. and Math. with Appl. 39 (5–6) (2000) 165–187.
[14] X.-Z. Liu, X. Cui, J.G. Sun, FDM for multi-dimensional nonlinear coupled system of parabolic and hyperbolic equations, J. Comput. Appl. Math. 186 (2) (2006) 432–449.
[15] H. Qin, D. Terzopoulos, D-NURBS: a physics-based framework for geometric design, IEEE Trans. Visualization and Comput. Graphics 2 (1) (1996) 85–96.
[16] R. Richtmyer, K. Morton, Difference Methods for Initial-Value Problem, second ed., Wiley-Interscience, New York, 1967.
[17] H. Ugail, M.I.G. Bloor, M.J. Wilson, Techniques for interactive design using the PDE method, ACM Trans. Graphics 18 (2) (1999) 195–212.
[18] W. Wesselink, R.C. Veltkamp, Interactive design of constrained variational curves, Comput. Aided Geom. Design 12 (5) (1995) 533–546.
[19] W.S. Zhang, L.J. Shen, Weak-implicit and explicit schemes for nonlinear wave equations, Math. Numer. Sinica 17 (2) (1995) 218–227.
[20] Y.L. Zhou, Applications of Discrete Functional Analysis to the Finite Difference Method, International Academic Publishers, Beijing, 1990.
[21] X.X. Zhu, The Modelling of Free-Form Curve and Surface, Science Press, Beijing, 2000.